2021 43rd Annual International Conference of the
IEEE Engineering in Medicine & Biology Society (EMBC)
Oct 31 - Nov 4, 2021. Virtual Conference

Cause of Subharmonics in Local Field Potentials Recorded by Sensing-Enabled Neurostimulator*

Yue Chen, Bozhi Ma, Hongwei Hao, and Luming Li

Abstract— **Sensing-enabled neurostimulators have become an essential technology for recording local field potentials (LFPs) during neurostimulation. However, subharmonics from indeterminate sources make interpreting LFP recordings a challenge. In this study, we investigated the characteristics and the cause of the subharmonics recorded by sensing-enabled neurostimulators. We found that the amplitudes and frequencies of the subharmonics in clinical LFPs varied with stimulation parameters. Using simulated solutions, we demonstrated that these subharmonics were device-generated noise. The cause of the subharmonics was the ripples in the stimulation pulses residual in the final LFP recordings. Our results provided a method to discriminate the subharmonic artifacts and suggested that interpretation of the subharmonics at a fractional frequency of stimulations in LFP recordings should be performed carefully.**

Clinical Relevance— **This study reveals the cause of subharmonics in LFP recordings for clinical neuroscience research.**

I. Introduction

Recently, sensing-enabled neurostimulators have emerged as a technology for synchronously recording local field potentials (LFPs) during stimulation [1]. It opened a window into long-term brain activity and paved the way for closed-loop deep brain stimulation (DBS) and brain-computer interfaces [2, 3]. However, acquiring faithful recordings during stimulation can be challenging. Residual stimulation artifacts could be more than two orders of magnitude greater than LFPs. Complex components from indeterminate sources could residue with stimulation artifacts, interfering with the ability to distinguish between neural activity and noise.

In LFP recordings, multiple components related to stimulation artifacts could be recognized, including those at fundamental stimulation frequency, multiplication frequencies, and aliasing frequencies. Among these components, subharmonics at fractional frequencies of the stimulation frequency are highly elusive. Previous studies using sensing-enabled neurostimulators reported several subharmonics in LFP recordings during 140Hz stimulation, including subharmonics around 70Hz [4, 5]. Subharmonics at other frequencies in the gamma, beta, and lower bands were also reported [6-8]. The subharmonics could not be fully explained by aliasing. Most of these studies regarded the subharmonics as noise and excluded them from analysis. Our previous study also found some subharmonics in the LFPs recorded by sensing-enabled neurostimulators [9]. We found the magnitudes and frequency of the subharmonics varied with stimulation parameters and across individuals. A lack of explanations regarding these subharmonics made it challenging to interpret the recordings of sensing-enabled neurostimulators, resulting in data wastage.

In this study, we systematically report the characteristics of the subharmonics in the LFPs recorded by the sensing-enabled neurostimulator and investigate the cause of the subharmonics. Using simulated solutions, we found that the subharmonics could be recorded in abiotic environments and demonstrated that these subharmonics were from the noise in the stimulation pulses.

II. Methods

A. Clinical LFP Acquisition

1) Subjects and DBS Implantation

To observe the characteristics of subharmonics, we collected LFPs in the subthalamic nucleus (STN) from DBS patients. The recordings were from the experiments in our previous studies [9, 10]. All the experimental procedures were approved by the local ethical committees and all the subjects provided written informed consent.

2) LFP Recording Parameters

LFPs were recorded by sensing-enabled neurostimulators. The electrode of the neurostimulators consisted of four platinum-iridium cylindrical contacts (Model L301C, PINS Medical, China). The contacts were 1.3mm in diameter, 1.5mm in length, and spaced 0.5mm apart. Extensions of the electrode were connected to the neurostimulator (G106R, PINS Medical, China). Signals were differentiated between a pair of contacts and filtered by a built-in 0.3-250Hz band-pass filter. The data was then synchronically transmitted to the recording platform through wireless radio-frequency communication. The sampling rate was 1000 Hz.

B. Simulated LFP Acquisition

To investigate the cause of the subharmonics, we set simulated environments to reproduce the LFP recording

*Research supported by the National Natural Science Foundation of China Grants 61901243, and the Shenzhen International Cooperative Research Project GJHZ20180930110402104.

Y. Chen is with the National Engineering laboratory for Neuromodulation, Tsinghua University, Beijing, China (e-mail: hellochenyue@foxmail.com).

B. Ma is with the National Engineering laboratory for Neuromodulation, Tsinghua University, Beijing, China (e-mail: mbz@tsinghua.edu.cn).

H. Hao is with the National Engineering laboratory for Neuromodulation, Tsinghua University, Beijing, China (e-mail: haohw@tsinghua.edu.cn).

Corresponding author: L. Li is with the National Engineering laboratory for Neuromodulation, Tsinghua University, Beijing, China (corresponding author, phone: +86-10-62785716; fax: +86-10-62785716; e-mail: lilm@mail.tsinghua.edu.cn). He is also with Precision Medicine & Healthcare Research Center (Tsinghua-Berkeley Shenzhen Institute, Tsinghua University, Shenzhen, China), IDG/McGovern Institute for Brain Research at Tsinghua University (Beijing, China), and Institute of Epilepsy, Beijing Institute for Brain Disorders (Beijing, China).

procedure. The simulated environments included a saline setup and a resistance network setup.

1) *Saline Simulation*

Fig. 1(a) shows the saline solution. A DBS electrode and an Ag/AgCl disc-electrode were fully immersed in a spherical glass container. The container was about 30cm in diameter and filled with normal saline (NaCl 0.9%). The DBS electrode was connected to a sensing-enabled neurostimulator. The Ag/AgCl disc-electrode was connected to the titanium case of the neurostimulator. Stimulation was delivered via Ag/AgCl electrode (anode) and contact 2 (cathode). Contacts 1 and 3 were used for recording. The sampling rate was 1000 Hz.

2) *Resistance Network Simulation*

Fig. 1(b) shows a resistance network used to simulate the electrode/tissue interface. R_c was connected to the titanium case of the neurostimulator. R_1, R_2, and R_3 were connected to contact 1, contact 2, and contact 3, respectively. Stimulation was delivered via the titanium case and contact 2. Contacts 1 and 3 were used for recording. The sampling rate was 1000 Hz.

C. Data Analysis

Spectrums were generated by short-time Fourier transforms. Power spectrum density (PSD) was calculated using Welch's method. The spectrum and PSD were calculated using the Hamming window of 1s and overlap of 0.75s. The frequency resolution of the spectrums was 1Hz.

III. Results

To study the cause of the subharmonics, we first investigated the characteristics of the subharmonics in clinical LFPs. Then we used saline and resistance network solutions to reproduce the subharmonics with similar characteristics. Lastly, the subharmonic source was traced in the chain from recording to stimulation circuits.

A. Characteristics of the Subharmonics in Clinical LFPs

Fig. 2 shows the spectrums of LFP recordings under different stimulation frequencies. In Fig. 2(a), stimulation was programmed from 60Hz to 180Hz with a step of 10Hz (2V, 90μs). The area between the two dashed black lines shows that the subharmonics followed the stimulation at a consistent fraction of 1/2. For example, in Fig. 2(b), the subharmonics located at 65Hz during 130Hz stimulation, and increased to 70Hz during 140Hz stimulation. Fig. 2(c) shows examples from another subject (3.0V, 90μs). Compared with Fig. 2(b), the subharmonic peaks became sharper at half the stimulation frequencies. These results indicated that the subharmonics might be located at a constant fractional frequency across the stimulation frequencies.

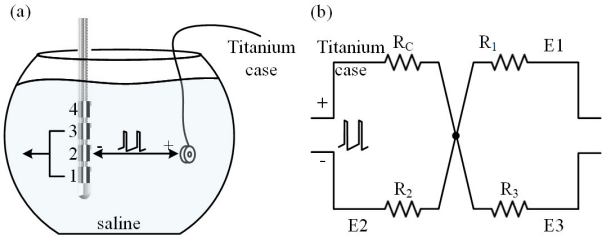

Figure 1. Illustration of the simulation setup. (a) Saline simulation. (b) Resistance-network simulation.

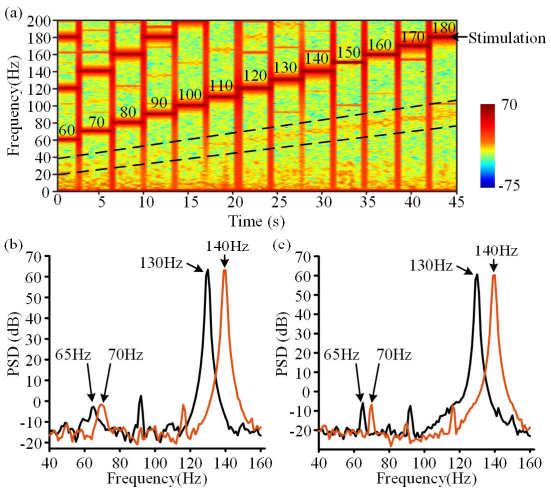

Figure 2. Subharmonics under different stimulation frequencies. (a). The spectrum. (b). PSDs in (a). (c) PSDs from another piece of recording.

However, the fractional frequency varied with stimulation amplitudes. Fig. 3 shows the LFP spectrums from three subjects under different stimulation amplitudes. In Fig. 3(a), stimulation was from 1.3V to 2.1V with a step of 0.1V (130Hz, 60μs). Subharmonics were found at one-fifth of the stimulation frequency during 1.3V stimulation and gradually increased to half the stimulation frequency during 1.4-2.1V. In Fig. 3(b), subharmonics were found during 2.6-3.0V stimulation (130Hz, 60μs) and the fractional frequency varied. Fig. 3(c) shows an example of subharmonics which only appeared during 1.9 and 2.0V stimulation (130Hz, 60μs).

These results show that the subharmonics varied with stimulation parameters. Stimulation amplitude influenced the fractional frequency and intensity of the subharmonics. Once the stimulation amplitude was fixed, the subharmonics, if there were any, followed the stimulation frequency at a consistent fractional frequency. Additionally, although a subgroup of the

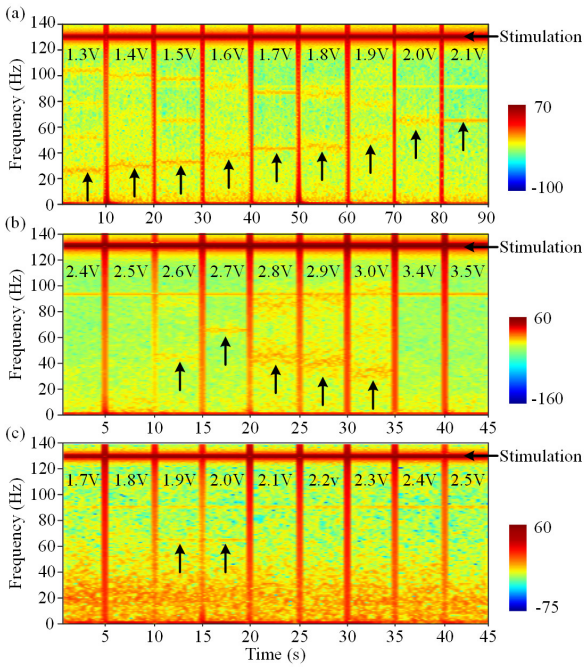

Figure 3. The spectrum of clinical LFPs under different stimulation amplitudes. The black arrows indexed the subharmonics.

stimulation parameters (1.7-2.1V) in Fig. 3(a and c) were similar, the subharmonics were significantly different. It seems that the subharmonics might randomly change across individuals or devices. Subharmonics with a fraction of 1/2 were most easily recorded in the LFPs. In some cases, no subharmonics could be found across stimulation amplitudes.

B. The Subharmonics Are Noise from the Neurostimulator

To figure out whether these subharmonics were physiological potentials or noise, we conducted simulated recording in a saline solution and resistance network.

1) *Subharmonics in the Saline Medium*

In Fig. 4, we recorded subharmonics (70Hz) at half the stimulation frequency (140Hz, 1V, 90μs) when the Ag/AgCl disc-electrode was positioned at one specific location (location 1). However, when we changed the horizontal distance between the Ag/AgCl disc-electrode and the DBS electrode (location 2), the subharmonics dispersed. This pattern was repeatable when the Ag/AgCl disc-electrode was restored to location 1. In most other locations, no subharmonics could be recorded. These results showed that the subharmonics could be recorded in the saline medium. However, the subharmonics were primarily affected by the relative distance of the stimulation electrodes. We did not find a relationship describing electrode location and induction of subharmonics.

2) *Subharmonics in the Resistance Network*

The different stimulation electrode locations brought about the different distributions of electrical field and load impedances in the saline medium. To exclude these uncertain variables, we further investigated the subharmonics using the resistance network. In Fig. 1(b), resistors R_c (100Ω) and R_2 (1kΩ) were the tissue load for the stimulation circuits. Resistors R_1 and R_3 were the tissue interface for the recording circuits. The match between R_1 and R_3 influenced the magnitude of the stimulation artifacts in the final recordings. Here we set R_1 to 1KΩ and R_3 to 1.9KΩ. Fig. 5(a) shows the spectrums of recordings under different stimulation amplitudes. Stimulation was programmed from 0.5V to1.25V with a step of 0.05V (130Hz, 90μs). Significant subharmonics appeared and were similar to the clinical LFPs in Fig. 3. Fig. 5(b) shows the subharmonics under stimulation from 60Hz to 180Hz with a step of 10Hz (1.1V, 90μs). The subharmonics located at a constant fraction (1/2) of the stimulation frequency were similar to those in Fig. 2. Fig. 5(c) shows the subharmonics under stimulation of 60μs. Compared with Fig. 5(a) (90μs), the fractional frequencies of the subharmonics shifted. Fig. 5(d) shows the subharmonics recorded after the R_2 was adjusted to 0.5kΩ and 1.5kΩ. Compared with Fig. 5(a) (R_2 was 1kΩ), the fractional frequency of the subharmonics shifted in two directions.

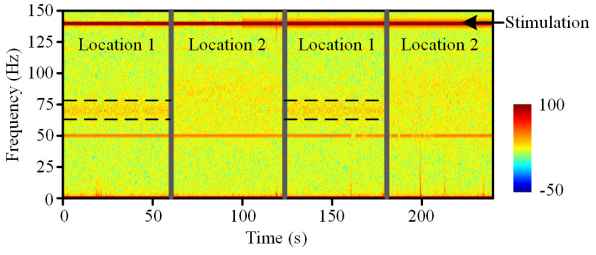

Figure 4. Subharmonics in saline recordings. Power frequency is 50Hz.

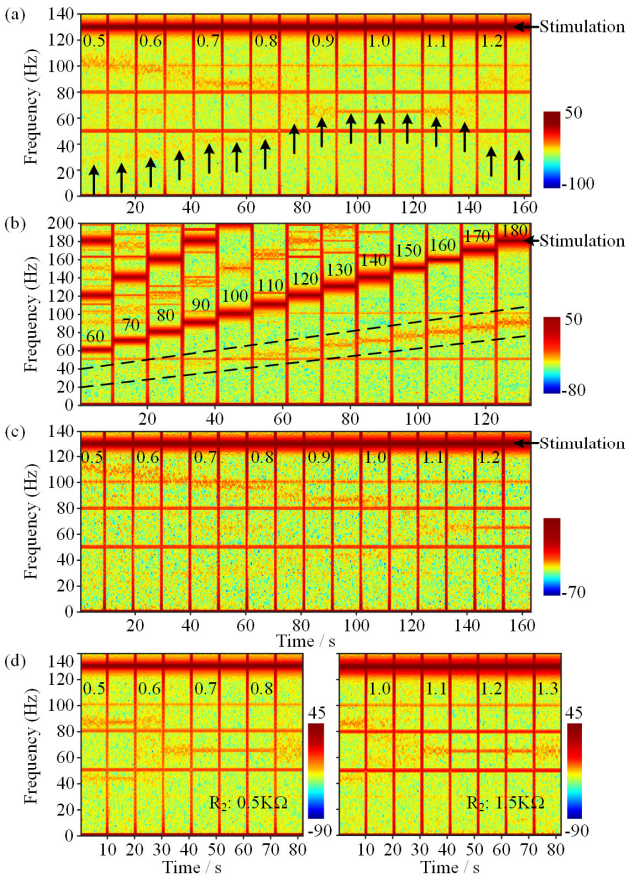

Figure 5. Subharmonics recorded with the resistance network under stimulation of (a) 0.5-1.25V (130Hz, 90μs), (b) 60-180Hz (1.1V, 90μs), and (c) 60μs (0.5V-1.25V, 130Hz). (d). R_2 was 0.5kΩ and 1.5kΩ. 50Hz, 100Hz, and 80Hz are the power frequency, its harmonic, and crossover frequency.

So far, we reproduced the subharmonics using the saline and resistance network. The subharmonics changed with the stimulation parameters and the load impedance of the stimulation circuit. Load impedance of the stimulation circuits, stimulation amplitudes, and pulse width shifted the fractional frequency of the subharmonics, while stimulation frequency did not. The magnitude of subharmonics with a fraction of 1/2 was higher. The results demonstrated that the subharmonics in LFP recordings were device-generated noise.

C. The Subharmonics Are from Stimulation Pulses

To investigate the subharmonic source, we traced the signals from the sampling module backward to the pulse generator using the resistance network. We found some ripples in the stimulation pulses that appeared with the subharmonics. The ripple frequency was strongly related to the fractional frequency of the subharmonics. For example, in Fig. 6(a), the ripples covered two stimulation pulses, and the subharmonics were at half the stimulation frequency in Fig. 5(a) (at 1.1V). In Fig. 6(b), most of the ripples covered three pulses, and the subharmonics were at one-third of the stimulation frequency in Fig. 5(a) (at 0.75V). In Fig. 6(c), most of the ripples covered four pulses, and the subharmonics were at one-fourth of the stimulation frequency in Fig. 5(a) (at 0.6V). These ripples were initially found in the stimulation pulses and existed in the following signal chain of the recording module.

Based on the above analysis, we updated the pulse generator circuits to reduce the ripples in the pulses.

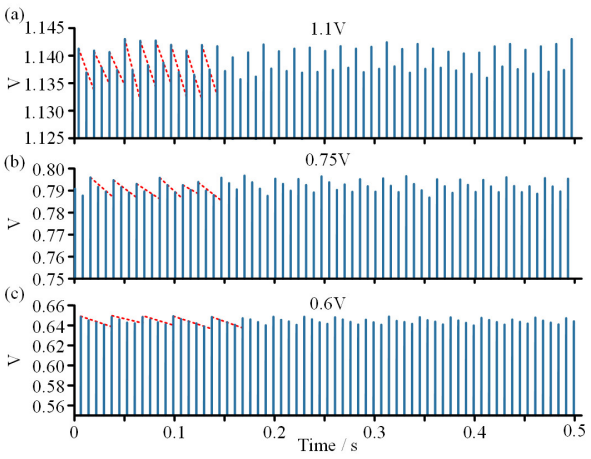

Figure 6. The source of the subharmonics in the stimulation pulses. Stimulation frequency was 130Hz, and the pulse width was 90μs. Stimulation amplitudes were 1.1V, 0.75V, and 0.6V.

Modifications of the circuits included output stabilization and power supply oscillation reduction. We use the optimized neurostimulator to record the simulated LFPs in the same resistance network under the stimulation parameters which were the same as in Fig. 5. Fig. 7 shows the spectrum of recordings. The results show that the subharmonics disappeared under all parameters after removing the ripples.

IV. Discussion

In this study, we investigated the subharmonics in LFPs recorded by sensing-enabled neurostimulators. By demonstrating the subharmonics were repeatable in abiotic environments, we confirmed that these subharmonics were residual noise in the stimulation pulses. The results would be helpful for researchers to discriminate the subharmonics artifacts with physiological signals.

Our results indicated that the source of the subharmonics was the ripples in the stimulation pulses. The peak-to-peak amplitudes of the ripples could be several mVs, which were similar to the strength of ECG influence. This magnitude would not influence clinical DBS effects, but could be residual in the LFP recordings. Our work suggested the generation of the ripples results from the nonlinearity of the circuits. Eliminating the nonlinearity of the stimulation circuits could largely improve the quality of LFP recording.

Several factors influence the subharmonics. Stimulation amplitude, pulse width, and the load impedance of the stimulation circuits could change the fractional frequency of the subharmonics. This is because these parameters changed the electric charge outputted within each pulse, leading to the different working rhythms of the output circuits. Stimulation

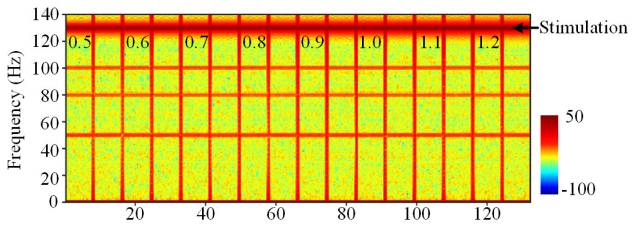

Figure 7. The subharmonics disappeared after ripples in the stimulation pulses were removed. Components of 50Hz, 100Hz, and 80Hz are the power frequency, its harmonic, and crossover frequency.

frequency did not change the electric charge outputted within each pulse., and so the fractional frequency of the subharmonics was consistent. In our study, the subharmonics recoded using the resistance network appeared at different stimulation parameters with those in clinical LFPs. This is primarily from the difference between the simulation load and the actual physiological environment. Future works should include capacitive components in the circuit simulation. Moreover, because the ripples are common-mode noise, factors that influence the common-mode rejection ratio of the recording chain would affect the strength of the subharmonics in the final LFP recordings. This also explained that it might be easier to record a subharmonic with half stimulation frequency (see Fig. 3) because the common-mode ripple is more concentrated in frequency domain. As a result of the combination of all the above factors, subharmonics could be elusive in LFP recordings, varying across stimulation parameters, individuals, and even implantation time. For the discrimination of subharmonic artifacts, we suggest a scan of LFP recording to inspect the subharmonic patterns under different stimulation parameters. The interpretation of the components at a fractional frequency of stimulations in LFP recordings should be performed carefully.

Acknowledgment

We thank Dr. Jianguo Zhang (Department of Neurosurgery, Beijing Tiantan Hospital of Capital Medical University), Dr. Yi Guo (Department of Neurosurgery, Peking Union Medical College Hospital), Dr. Shujun Xu (Department of Neurosurgery, Qilu Hospital of Shandong University), and their team for the help in clinical experiments.

References

[1] H. Shen, "Neuroscience: Tuning the brain," *Nature,* N/OL vol. 507, pp. 290-292, 2014-03-19 2014.

[2] A. Velisar *et al.*, "Dual threshold neural closed loop deep brain stimulation in Parkinson disease patients," *Brain Stimul.,* vol. 12, no. 4, pp. 868-876, 2019.

[3] H. M. Golshan, A. O. Hebb, and M. H. Mahoor, "LFP-Net: A deep learning framework to recognize human behavioral activities using brain STN-LFP signals," *J. Neurosci. Methods,* vol. 335, p. 108621, 2020.

[4] E. J. Quinn *et al.*, "Beta oscillations in freely moving Parkinson's subjects are attenuated during deep brain stimulation," *Mov. Disord.,* vol. 30, no. 13, pp. 1750-1758, 2015.

[5] W. J. Neumann *et al.*, "Deep Brain Recordings Using an Implanted Pulse Generator in Parkinson's Disease," *Neuromodulation,* vol. 19, no. 1, pp. 20-24, 2016.

[6] A. A. Kühn *et al.*, "High-frequency stimulation of the subthalamic nucleus suppresses oscillatory β activity in patients with Parkinson's disease in parallel with improvement in motor performance," *J. Neurosci.,* vol. 28, no. 24, pp. 6165-6173, 2008.

[7] P. H. Stypulkowski, S. R. Stanslaski, T. J. Denison, and J. E. Giftakis, "Chronic evaluation of a clinical system for deep brain stimulation and recording of neural network activity," *Stereotact. Funct. Neurosurg.,* vol. 91, no. 4, pp. 220-232, 2013.

[8] K. Airaksinen *et al.*, "Cortico-muscular coherence in advanced Parkinson's disease with deep brain stimulation," *Clin. Neurophysiol.,* vol. 126, no. 4, pp. 748-755, 2015.

[9] Y. Chen *et al.*, "Neuromodulation effects of deep brain stimulation on beta rhythm: A longitudinal local field potential study," *Brain Stimul.,* vol. 13, no. 6, pp. 1784-1792, 2020.

[10] X. Qian, Y. Chen, Y. Feng, B. Ma, H. Hao, and L. Li, "A method for removal of deep brain stimulation artifact from local field potentials," *IEEE Trans. Neural Syst. Rehabil. Eng.,* vol. 25, no. 12, pp. 2217-2226, 2017.